Biophysical Chemistry, 34 (1989) 91-102
Elsevier

BIOCHE 01375

Irreversible thermodynamic model equations of the transport across a horizontally mounted membrane

A. Ślęzak

Department of Biophysics, Silesian Medical Academy, Karol Marx Str. 19, 41-808 Zabrze 8, Poland

Received 21 September 1987
Revised manuscript received 12 December 1988
Accepted 16 May 1989

Membrane transport; Kedem-Katchalsky-Zelman model

The Kedem-Katchalsky-Zelman model equations for transmembrane transport in multicomponent, non-ionic and heterogeneous solutions have been modified. The validity of this model for binary and ternary solutions was verified, using a cell with a horizontally mounted membrane. In the cell, volume and solute fluxes were measured as a function of gravitational configuration. In the experimental set-up, water was placed on one side of the membrane. The opposite side of the membrane was exposed to aqueous solutions of densities greater than that of water, aqueous ethanol (less dense than water) or glucose/ethanol/water solutions. The experimental results presented herein illustrate pseudo-phase transitions which occur from a non-convectional to convectional state or in the reverse direction.

1. Introduction

The mathematical models of transmembrane transport currently in existence introduce the proper equations of transport, consisting first of all of readily measured parameters characterizing the membrane. Thus far, several mathematical models of transmembrane transport are known. The oldest is that based on the equations of Fick's diffusion model [1], as adapted for a description of membrane phenomena [2,3]. Among the most recent are those which have been elaborated on the grounds of statistical mechanics, based on the equations of the Nernst-Planck and Stephan-Maxwell diffusion model [4-8], the Spiegler-Kedem-Katchalsky frictional model, [9,10], and irreversible thermodynamics, particularly Onsager's laws [11]. Among the models based on thermodynamics, the equations of the Kedem-Katchalsky non-equilibrium thermodynamic model are of great importance [12-16]. They are used for the interpretation of membrane phenomena occurring in model membrane systems and also in systems containing biological membranes [2,17].

The first analysis of transmembrane transport on the basis of non-equilibrium thermodynamics was performed by Staverman [18]. However, the papers of Kedem and Katchalsky [10-16], Zelman [19], Richardson et al. [20] and Del Castillo and Mason [21] have devised cohesive models of membrane transport.

We shall restrict ourselves to the Kedem-Katchalsky transmembrane transport equations, generalized by Zelman [19] for multicomponent solutions, which are determined by the Kedem-Katchalsky-Zelman model equations of transmembrane transport (KKZ model). This model can be written in the following form

$$J_v = L_p\Big(\Delta P \pm \sum_k \sigma_k\, \Delta\Pi_k\Big), \tag{1}$$

$$J_s = J_v(1-\sigma_s)\bar{C}_s + \sum_k \omega_{ks}\, \Delta\Pi_k, \tag{2}$$

Correspondence address: A. Ślęzak, Department of Biophysics, Silesian Medical Academy, Karol Marx Str. 19, 41-808 Zabrze 8, Poland.

where J_v and J_s are the volume and solute fluxes, respectively, L_p the hydraulic conductivity of the membrane, ΔP the hydrostatic pressure difference, $\bar{C}_s$ the average solute concentration, σ_k and σ_s the reflection coefficients of the membrane for the k-th and s-th substances, respectively, $\Delta\Pi_k$ and $\Delta\Pi_s$ the osmotic pressure differences for the k-th and s-th substances, respectively, ω_{ks} the permeability of the s-th substance, which passes across the membrane under the influence of the gradient of the k-th substance osmotic pressure difference ($\omega_{ks} = \omega_{sk}\bar{C}_s/\bar{C}_k$) and s, $k = 1, 2, \ldots, n$, $s = k$; the $(n+1)$-th component is the solvent for which $\sigma_{n+1} = 0$.

Application of the existing mathematical models of transport across membranes (including the KKZ model) is limited to the case where the phases separating the membrane are homogeneous (equally stirred). Therefore, no reference is made with respect to the case in which additional phases, termed boundary layers, occur on both sides of the membrane in model membrane and biological systems [22–30]. The boundary layers produced on both sides of a membrane mounted horizontally with respect to the gravitational field, determine the group of membrane phenomena which include the graviosmosis and gravielectric effects [31–40]. In general, these phenomena appear when: (i) a concentration gradient is produced on the selectivity membrane or series of membranes; (ii) the density gradient is produced in the phases separated by the membrane; and (iii) the density gradient (parallel or antiparallel to the vector of gravity) is perpendicular to the membrane or series of membranes.

Studies on gravity-induced transport in single-membrane systems were initiated by Brauner [37] who discovered the gravielectric effect. These investigations were continued by others [38–40]. From previous papers [27–30,41] and the present article, the conclusion is drawn that the influence of the gravitational field on transmembrane transport manifests itself in asymmetry and amplification of osmotic, diffusive [30,41] and graviosmotic [31–36,50] transport, and Rayleigh-Taylor instability [27,28].

Up to now there has been no suitable mathematical formalism, which could describe the dynamics of the flows across the membrane especially with respect to gravity-induced membrane phenomena.

With this in mind, in the present paper a suitable formalism based on the KKZ model equations [12,19] is presented. In order to verify the formalism, the results of experimental studies upon osmotic and diffusive transport in a single-membrane system containing binary and ternary solutions are presented.

2. Modification of the Kedem-Katchalsky-Zelman model equations

It was proved [22–30] that, as a result of the mass transport across a membrane separating liquids of different compositions, boundary layers are invariably produced. These are regions in the external liquids, adjacent to membrane interfaces, where concentration gradients are maintained under steady-state conditions. The boundary layers act as pseudo-membranes in series with the physical membrane. Consequently, they can cause substantial reductions in the transmembrane flux. Vigorous mechanical stirring of the external liquids minimizes the boundary layer thickness and flux reduction.

Let us consider the membrane system represented in fig. 1. We assume that this membrane system contains heterogeneous, n-component solutions (not mechanically stirred). In this system, at steady state, boundary layers are formed on both sides of the membrane. The remaining assumptions are analogous to those in the case of homogeneous solutions [13]. The implication from the above is that the concentrations of solutions at the boundaries between the membrane and the layers are different from those at the boundaries between the membrane and stirred solutions. We denote the former concentrations by c_1^{I}, c_1^{II}, c_2^{I}, $c_2^{\mathrm{II}}, \ldots$, c_n^{I}, c_n^{II}, respectively, while the concentrations outside the boundaries are designated C_1^{I}, C_1^{II}, C_2^{I}, $C_2^{\mathrm{II}}, \ldots$, C_n^{I}, C_n^{II}. The reflection and permeability coefficients of the membrane for the s-th substance are denoted by σ_s and ω_s, respectively, and solute flux by j_s. The solute flux across the boundary layer/membrane/boundary layer

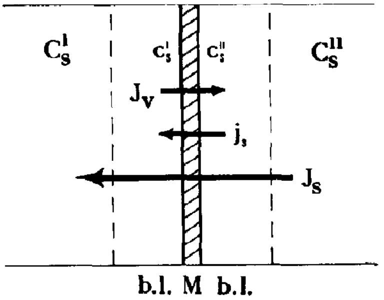

Fig. 1. Membrane system in which the membrane (M) separates two heterogeneous n-component solutions; C_s^I and C_s^{II}, global solution concentrations; c_s^I and c_s^{II}, local (at boundaries between membrane and boundary layers) solution concentrations; J_v^*, volume flux; j_s, solute flux across the membrane; J_s^*, solute flux across the complex b.l./M/b.l.; b.l., boundary layer.

(b.l./M/b.l.) complex is denoted by J_s^*, the reflection and permeability coefficients by σ_s^* and Ω, respectively.

For the case presented in fig. 1 we can write Van't Hoff's law as follows:

$$\Delta\pi = RT\,\Delta c_s, \tag{3}$$

$$\Delta\Pi = RT\,\Delta C_s,\ s = 1, 2, \ldots, n, \tag{4}$$

Eqs. 1 and 2, describing volume and solute fluxes respectively, can be written alternatively as:

$$J_v^* = L_p\Big(\Delta P \pm \sum_k \sigma_k\,\Delta\pi_k\Big), \tag{5}$$

$$j_s = J_v^*(1-\sigma_s)\bar{c}_s + \sum_k \omega_{ks}\,\Delta\Pi_k, \tag{6}$$

$$J_s^* = J_v^*(1-\sigma_s^*)\bar{C}_s + \sum_k \Omega_{ks}\,\Delta\Pi_k, \tag{7}$$

where s, $k = 1, 2, \ldots, n$ and $s \neq k$.
At steady state, the following conditions are fulfilled

$$J_s = j_s = J_s^*$$

and

$$\bar{C}_s = \bar{c}_s = \bar{C}_s^*. \tag{8}$$

Combining eqs. 5–7 we obtain n equations of the following type

$$\sum_k \omega_{ks}\,\Delta\pi_k = \sum_k \Omega_{ks}\,\Delta\Pi_k + J_v^*(\sigma_s - \sigma_s^*)\bar{C}_s^*. \tag{9}$$

Introducing the permeability tensor of the membrane ($\boldsymbol{K}$), the system of equations (eq. 9) can be written as

$$\boldsymbol{K}\begin{bmatrix}\Delta\pi_1\\ \vdots\\ \Delta\pi_n\end{bmatrix} = \begin{bmatrix}\sum_k \Omega_{k1}\,\Delta\Pi_k + J_v^*(\sigma_1 - \sigma_1^*)\bar{C}_1\\ \cdots\cdots\cdots\cdots\cdots\cdots\\ \sum_k \Omega_{kn}\,\Delta\Pi_n + J_v^*(\sigma_n - \sigma_n^*)\bar{C}_n\end{bmatrix} \equiv \mathscr{L} \tag{10}$$

where

$$\boldsymbol{K} \equiv \begin{bmatrix}\omega_{11},\ \omega_{21}, \ldots, \omega_{n1}\\ \cdots\cdots\cdots\cdots\\ \omega_{1n},\ \omega_{2n}, \ldots, \omega_{nn}\end{bmatrix}$$

If we designate the tensor, formed by substituting the i-th column by the vector $\mathscr{L}$, as $\boldsymbol{K}_i$, we can write an expression relating the osmotic pressure difference on both sides of the membrane with that on both sides of the complex (b.l./M/b.l.), namely

$$\Delta\pi_i = \frac{\det K_i}{\det K} \tag{11}$$

where

$$\boldsymbol{K}_i \equiv \begin{bmatrix} \overset{i}{\omega_{11}, \ldots, \ldots, \ldots, \omega_{n1}}\\ \cdot\\ \mathscr{L}\\ \cdot\\ \omega_{1n}, \ldots, \ldots, \ldots, \omega_{nn}\end{bmatrix}$$

Regarding the properties of the determinants we can write

$$\det K_i = \det K_i + J_v^* \det M_i, \tag{12}$$

where

$$\boldsymbol{M}_i \equiv \begin{bmatrix}\omega_{11}, \ldots, \omega_{i-1,1},\ \bar{C}_1^*(\sigma_1 - \sigma_1^*),\ \omega_{i+1,1}, \ldots, \omega_{n1}\\ \cdots\cdots\cdots\cdots\cdots\cdots\cdots\cdots\\ \omega_{1n}, \ldots, \omega_{i-1,1},\ \bar{C}_n^*(\sigma_n - \sigma_n^*),\ \omega_{i+1,1}, \ldots, \omega_{nn}\end{bmatrix}$$

In analogy with eq. 10, we can write

$$\det K_i = \sum_k \Delta\Pi_k \det K_{ik}, \tag{13}$$

where

$$\boldsymbol{K}_{ik} \equiv \begin{bmatrix}\omega_{11}, \ldots, \omega_{i-1,1},\ \Omega_{k1},\ \omega_{i+1,1}, \ldots, \omega_{n1}\\ \cdots\cdots\cdots\cdots\cdots\cdots\cdots\\ \omega_{1n}, \ldots, \omega_{i-1,n},\ \Omega_{kn},\ \omega_{i+1,n}, \ldots, \omega_{nn}\end{bmatrix}$$

is a tensor formed by replacement of the i-th column in tensor $\boldsymbol{K}$, by the column of the permeability coefficients Ω_{kj}. With the aid of eqs. 11 and 12

$$\det K_i = \sum_k \Delta\Pi_k \det K_{ik} + J_v^* \det M_i. \tag{14}$$

Combining eqs. 13 and 14 we obtain

$$\Delta\pi_i = \frac{1}{\det K}\left[\sum_k \Delta\Pi_k \det K_{ik} + J_v^* \det M_i\right]. \tag{15}$$

Finally, a comparison between eqs. 5–7 and eq. 15 gives

$$J_v^* = L_p\left(\Delta P \pm \frac{1}{\det K}\sum_i \sigma_i \sum_k \Delta\Pi_k \det K_{ik}\right) \times \left(1 \mp \frac{1}{\det K} L_p \sum_i \sigma_i \det M_i\right)^{-1}, \tag{16}$$

$$J_s^* = J_v^* \bar{C}_s^* (1 - \sigma_s^*) + \frac{1}{\det K}\sum_i \omega_{is} \det M_i + \frac{1}{\det K}\sum_i \omega_{is} \sum_k \Delta\Pi_k \det K_{ik}. \tag{17}$$

Now, let us take into consideration the following relations

$$\frac{1}{\det K}\sum_i \omega_{is} \det M_i = \bar{C}_s^* (\sigma_s - \sigma_s^*), \tag{18}$$

$$\frac{1}{\det K}\sum_i \omega_{is} \sum_k \Delta\Pi_k \det K_{ik} = \sum_i \Omega_{is}\, \Delta\Pi_i. \tag{19}$$

The mathematical proof of these relations is presented in a previous paper [42].

In turn, using eqs. 18 and 19, eq. 18 can be written as

$$J_s^* = J_v^* \bar{C}_s^* (1 - \sigma_s^*) + \sum_i \Omega_{is} \Delta\Pi_i. \tag{20}$$

Eqs. 16 and 20 represent generalization of the Kedem-Katchalsky-Zelman model equations of transmembrane transport in multicomponent, non-ionic and heterogeneous solutions. These equations can be considered as a generalization of the transmembrane transport equations.

Discussion of these equations leads to the following conclusions:

(1) If we assume that $\omega_s = \Omega_s$ and $\sigma_s = \sigma_s^*$, which gives the condition

$$\frac{\det K_{ik}}{\det K} = \delta_{ki} \tag{21}$$

eqs. 16 and 20 transform into eqs. 1 and 2.

(2) If we assume that $n = 1$ in eqs. 16 and 20 we obtain the classical modification of the Kedem-Katchalsky equations

$$J_v^* = L_p\left\{\Delta P \pm \frac{\Omega_{11}}{\omega_{11}}\sigma_1\, \Delta\Pi_1\right\} \times \left\{\frac{\omega_{11}}{\omega_{11} \mp L_p \sigma_1 \bar{C}(\sigma_1^* - \sigma_1)}\right\}, \tag{22}$$

$$J_1^* = \Omega_{11}\, \Delta\Pi_1 + J_v^* (1 - \sigma_1^*) \bar{C}_1. \tag{23}$$

The above equations and their discussion were presented in a previous paper [29].

(3) If we assume that $n = 2$ in eqs. 16 and 20, we obtain the modification of the Kedem-Katchalsky-Zelman model equations for ternary solutions

$$J_v^* = \eta L_p\left\{\Delta P \pm \frac{1}{\det K}(\sigma_1 \det K_{11} + \sigma_2 \det K_{21}) \times \Delta\Pi_1 - (\sigma_1 \det K_{12} + \sigma_2 \det K_{22})\, \Delta\Pi_2\right\}, \tag{24}$$

$$J_1^* = J_v^* (1 - \sigma_1^*) \bar{C}_1^* + \Omega_{11}\, \Delta\Pi_1 + \Omega_{21}\, \Delta\Pi_2, \tag{25}$$

$$J_2^* = J_v^* (1 - \sigma_2^*) \bar{C}_2^* + \Omega_{12}\, \Delta\Pi_1 + \Omega_{22}\, \Delta\Pi_2, \tag{26}$$

where

$$\eta \equiv \left\{1 \mp L_p (\det K)^{-1} [\sigma_1 \det M_1 + \sigma_2 \det M_2]\right\}^{-1}.$$

In previous papers [41,42], eqs. 24–26 were experimentally verified for vertically mounted membranes. In the present paper, these equations will be experimentally verified for horizontally mounted membranes.

3. Experimental

3.1. Materials and methods

Studies upon quasi-stationary osmotic flows were carried out by means of methods of measurements that have been described in detail in previous papers [27,29,30]. In experiments, we used a nephron membrane (additional information about the membrane presented in ref. 29) and aqueous glucose and/or ethanol solutions.

Each experiment was performed for two gravitational configurations of the membrane system:

(a) with water in the vessel above the membrane and the solution below (configuration A),
(b) with the solution in the vessel above the membrane and water below (configuration B).

Measurements of J_v^* and J_s^* for both configurations were performed according to the following procedure. Firstly, determination of the value of J_v^* or J_s^* under conditions of thorough mechanical stirring of solutions is performed. For these experiments the steady state was observed after 10 min. Mechanical stirring of solutions was stopped after 1 h. In the next step measurements were carried out under conditions of no mechanical stirring of solutions over 5 h.

Evaluation of the global concentration exchanges in the solutions studied was performed by the standard isotope method. Details of this method have been published previously [13]. The measured value of the global concentration exchanges (dC) was used to calculate the solute flux (J_s^*) on the basis of the following equation

$$J_s = \frac{\mathrm{d}CV_c}{S\,\Delta t}, \tag{27}$$

where V_c is the volume of the measuring vessel.

The concentration dependences J_v and J_s were determined on the basis of time-dependent variability of J_v and J_s chosen by consideration of the values of J_v and J_s at steady state, obtained for different solution concentrations of the same substance. Each series of measurements was repeated four to seven times.

4. Results

4.1. Time dependences of J_v and J_s

A typical plot of the time dependence for J_v in configurations A and B of the membrane system in the case of a 0.1 M aqueous glucose solution and a nephron membrane was presented in a previous paper [45]. In fig. 2, an analogous plot for the dependence upon time of J_s is presented. Curve c, common for both configurations, contains the experimental results obtained under conditions of thorough mechanical stirring at 500 rpm, and shows that J_s is independent of the gravitational configuration of the membrane system. Traces b and a, obtained for configurations B and A, respectively, demonstrate that the J_s values for both configurations differ ($J_{sa} \neq J_{sb}$). It should be borne in mind that these dependences are quantitatively similar to the analogous dependences of J_v and the relation between J_{sc}, J_{sb} and J_{sa} is analogous to that for J_{vc}, J_{vb} and J_{va}.

In order to illustrate the dependence of the volume flux on the gravitational configuration, the time-dependent volume flux in two different gravitational configurations is presented in fig. 3. In the first experiment, an aqueous solution of glucose (curve 1A) or ethanol (curve 2A) was present in the compartment above the membrane, water being in the lower compartment. In the second experiment, in turn, the upper compartment contained water and the lower one an aque-

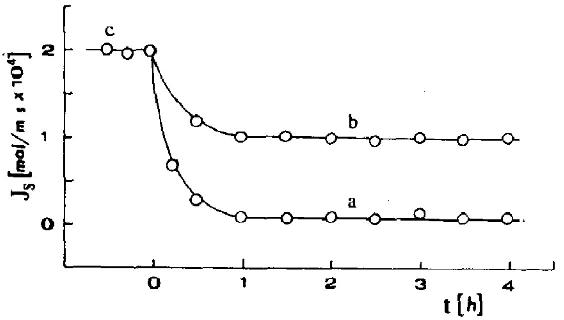

Fig. 2. Results on solute flux (J_s) as a function of time. Curve c was obtained for a system with mechanically stirred solutions; curves a and b for a membrane system without mechanical stirring of the solutions.

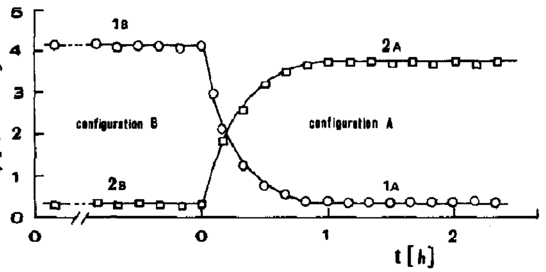

Fig. 3. Volume flux across the cell membrane as a function of time in two gravitational configurations for 0.1 M aqueous glucose solution (curve 1) and 0.3 M aqueous ethanol solution (curve 2). Curves 1A and 2A refer to configuration A; 1B and 2B, to configuration B.

ous solution of glucose (curve 1B) or ethanol (curve 2B).

In a previous paper [27], it was shown that water/glucose solutions have a higher density than pure water. In contrast, water is more dense than ethanol/water solutions. Consequently, the volume flux was greater when the upper compartment contained the denser fluid. The osmotic pressure gradient generated a volume flux directed from water towards the solutions in every case, irrespective of the gravitational configuration. An analogous picture was obtained for the solute flux (J_s^*). However, in this case the solute flux was directed from the solute toward water.

4.2. Characteristics of ternary solutions

Binary solutions can be divided into two groups (with regard to their density), under isothermal conditions. The first category includes solutions whose density is inversely proportional to their concentration; examples belonging to this group are aqueous solutions of the first-row alcohols (methanol, ethanol, etc.) and ammonia. The second consists of solutions whose density is proportional to their concentration; this group comprises solutions not belonging to the first group.

In contrast to binary solutions, the density of ternary solutions, composed of solvent, and of substances causing increased and decreased density of solutions (i.e., glucose and ethanol, respectively) may be lower than, equal to or greater than that of the solvent. Suitable experimental data were reported in the previous paper [27].

4.3. Concentration dependences J_v^* and J_s^* for ternary solutions

The trend followed by binary solutions (see fig. 3) is also valid for ternary glucose/ethanol/water solutions in the cell membrane compartment opposite to the compartment filled with water. Figs. 4 and 5 depict experimental data for J_v^* with respect to composition. The results in fig. 4 were obtained with solutions of fixed ethanol content and varying glucose concentration. For solutions containing 0.2 and 0.4 M ethanol, progressive addition of glucose increases the density from below that of water to a value above. Fig. 5 gives results at constant glucose and variable ethanol concentration. Here, progressive ethanol addition

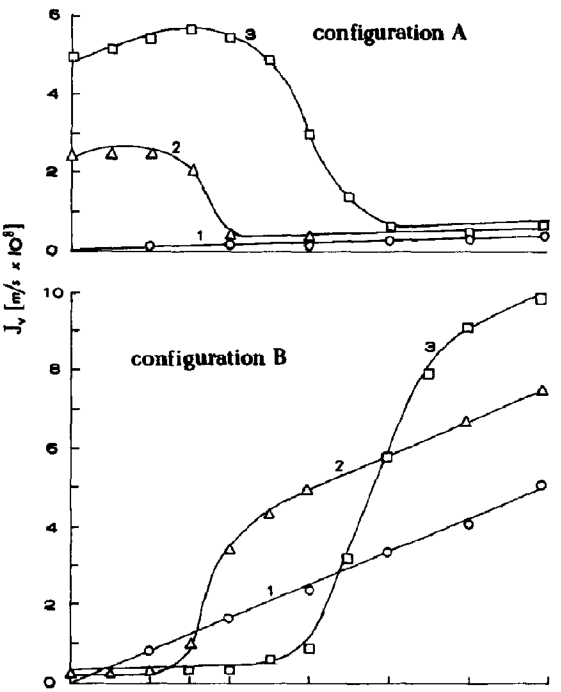

Fig. 4. Experimental and calculated volume flux across a cell membrane as a function of the glucose concentration difference for configuration A (upper) and B (lower): (○) no ethanol, (△) 0.2 M ethanol, (□) 0.4 M ethanol. Solid lines illustrate the volume flux calculated on the basis of eq. 26 after taking into consideration $\Omega_{11}(\Delta C_g)$ and $\Omega_{22}(\Delta C_g)$.

to 0.02 and 0.04 M glucose lowers the density from above to that of water a value below. The arrows in figs. 4 and 5 indicate those ternary compositions whose densities match that of water. Significantly, substantial volume flux changes occur at these values. In ref. 27, the manner in which J_v^* varies is related to the gravitational instability or stability of the boundary layers, i.e., if the experimental value of J_v^* is low, the boundary layers are stable and, conversely, for high values of J_v^*, the layers are unstable.

Figs. 6 and 7 display plots of the experimental data for ternary solutions. These results were obtained under conditions analogous to those for J_v^* (see figs. 4 and 5). The results in fig. 6 were obtained using solutions of constant ethanol concentration (0.2 and 0.4 M, respectively) while varying that of glucose. The results in fig. 7 correspond to the reverse of this situation, i.e., fixed glucose (0.02 and 0.04 M, respectively) and varying ethanol concentration. Suitable values of J_s^*, in analogy with J_v^*, can be interpreted in terms of a convective gravitational instability or stability of the boundary layers.

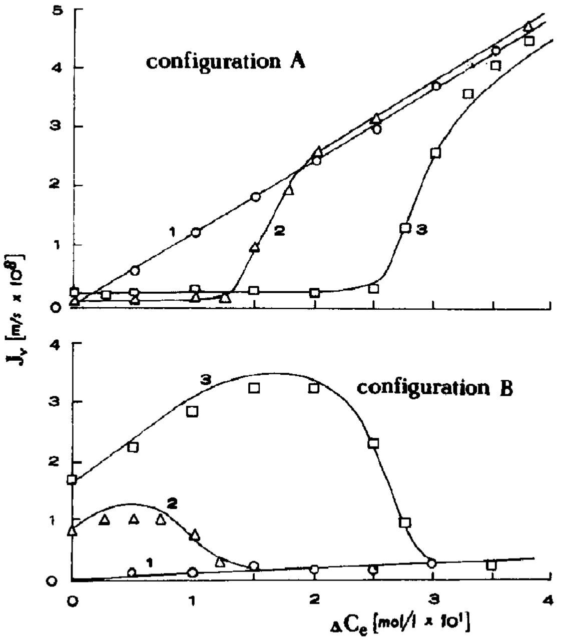

Fig. 5. Experimental and calculated volume flux across cell membranes as a function of ethanol concentration difference: (○) no glucose, (△) 0.02 M glucose, (□) 0.04 M glucose. Solid lines illustrate the volume flux calculated on the basis of eq. 26 after taking into consideration $\Omega_{22}(\Delta C_e)$ and $\Omega_{11}(\Delta C_e)$.

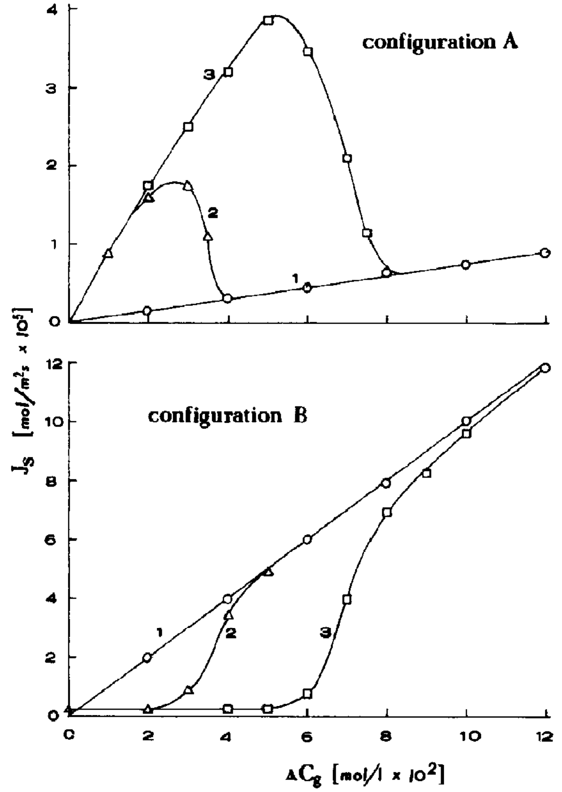

Fig. 6. Experimental and calculated glucose flux across cell membranes as a function of the glucose concentration difference. Experiments were performed under conditions analogous to those for the case of J_v^* (see fig. 4). Solid lines illustrate the solute flux calculated on the basis of eq. 27 after taking into consideration $\Omega_{11}(\Delta C_g)$.

5. Discussion

It appears from eqs. 22–26 that, in order to characterize the permeability properties of a horizontally mounted membrane for ternary solutions, 19 coefficients are needed in practice. These parameters are defined by the expressions listed in table 1, the corresponding values being detailed in table 2. It appears from the results in table 2 and from eqs. 24–26 that the values of the fluxes J_v^*

Table 1

Practical interpretation of membrane phenomenological parameters (L_p, σ, σ^*, ω, Ω)

Coefficient	Definition			
L_p	$L_p = (\frac{J_v}{\Delta P})_{\Delta\Pi_1,\Delta\Pi_2=0}$			
σ	$\sigma_1 = (\frac{\Delta P_1}{\Delta\Pi_1})_{J_v,\Delta\Pi_2=0}$	$\sigma_2 = (\frac{\Delta P_2}{\Delta\Pi_2})_{J_v,\Delta\Pi_1=0}$		
σ^*	$\sigma_1^* = (\frac{\Delta P_1^*}{\Delta\Pi_1})_{J_v,\Delta\Pi_2=0}$	$\sigma_2^* = (\frac{\Delta P_2^*}{\Delta\Pi_2})_{J_v,\Delta\Pi_1=0}$		
ω	$\omega_{11} = (\frac{J_1}{\Delta\Pi_1})_{J_v,\Delta\Pi_2=0}$	$\omega_{22} = (\frac{J_2}{\Delta\Pi_2})_{J_v,\Delta\Pi_1=0}$	$\omega_{12} = (\frac{J_1}{\Delta\Pi_2})_{J_v,\Delta\Pi_1=0}$	$\omega_{21} = (\frac{J_2}{\Delta\Pi_1})_{J_v,\Delta\Pi_2=0}$
Ω	$\Omega_{11} = (\frac{J_1^*}{\Delta\Pi_1})_{J_v,\Delta\Pi_2=0}$	$\Omega_{22} = (\frac{J_2^*}{\Delta\Pi_2})_{J_v,\Delta\Pi_1=0}$	$\Omega_{12} = (\frac{J_1^*}{\Delta\Pi_2})_{J_v,\Delta\Pi_1=0}$	$\Omega_{21} = (\frac{J_2^*}{\Delta\Pi_1})_{J_v,\Delta\Pi_2=0}$

and J_s^* are determined by the diagonal coefficients. Let us consider the coefficients ω_{ik} and Ω_{ik}. The diagonal coefficients are greater than the non-diagonal coefficients by three orders of magnitude. Thus, this provides the basis of reduction of eqs. 24–26 accepting $\omega_{12} = \omega_{21} = \Omega_{12} = \Omega_{21} \approx 0$. Regarding the above condition, and the results presented in figs. 8 and 9, eqs. 24–26 can be rewritten as

$$J_v^* = \eta\left[\Delta P \pm RT\frac{\Omega_{11}(C_1)}{\omega_{11}}\sigma_1\,\Delta C_1 - \frac{\Omega_{22}(C_2)}{\omega_{22}}\sigma_2\,\Delta C_2\right], \tag{28}$$

$$J_1^* = J_v^*(1-\sigma_1^*)\bar{C}_1 + \Omega_{11}(C_1)RT\,\Delta C_1, \tag{29}$$

$$J_2^* = J_v^*(1-\sigma_2^*)\bar{C}_2 + \Omega_{22}(C_2)RT\,\Delta C_2, \tag{30}$$

where

$$\eta = L_p\left\{1 \mp (\omega_{11}\omega_{22})^{-1}L_p\left[\sigma_{122}\bar{C}_1(\sigma_1-\sigma_1^*) + \sigma_2\omega_{11}\bar{C}_2(\sigma_2-\sigma_2^*)\right]\right\}^{-1}$$

$$RT\,\Delta C_1 = \Delta\Pi_1,$$

$$RT\,\Delta C_2 = \Delta\Pi_2.$$

We have obtained equations, including parameters (Ω) which refer to boundary layers. The equations can be used to analyse transmembrane transport across a horizontally mounted membrane in

Table 2

Values of the nephron membrane transport parameters for glucose (subscript 1) and ethanol (subscript 2)

Coefficient	Value of parameter	
	Configuration A	Configuration B
L_p (m^3/N per s) ($\times 10^{12}$)	5.0 ±0.2	5.0 ±0.2
σ_1 ($\times 10^2$)	6.8 ±0.2	6.8 ±0.2
σ_2 ($\times 10^2$)	2.5 ±0.1	2.5 ±0.1
σ_1^* ($\times 10^2$)	0.24±0.01	3.4 ±0.1
σ_2^* ($\times 10^2$)	1.0 ±0.04	0.1 ±0.01
ω_{11} (mol/N per s) ($\times 10^{10}$)	8.0 ±0.3	8.0 ±0.3
ω_{22} (mol/N per s) ($\times 10^{10}$)	2.0 ±0.08	2.0 ±0.08
ω_{12} (mol/N per s) ($\times 10^{13}$)	8.1 ±3.5	8.1 ±3.5
ω_{21} (mol/N per s) ($\times 10^{12}$)	1.63±0.6	1.63±0.6
Ω_{11} (mol/N per s) ($\times 10^{10}$)	0.3 ±0.04	4.0 ±0.2
Ω_{22} (mol/N per s) ($\times 10^{10}$)	1.0 ±0.06	0.06±0.02
Ω_{12} (mol/N per s) ($\times 10^{13}$)	0.85±0.3	0.07±0.05
Ω_{21} (mol/N per s) ($\times 10^{12}$)	0.4 ±0.3	4.0 ±0.8

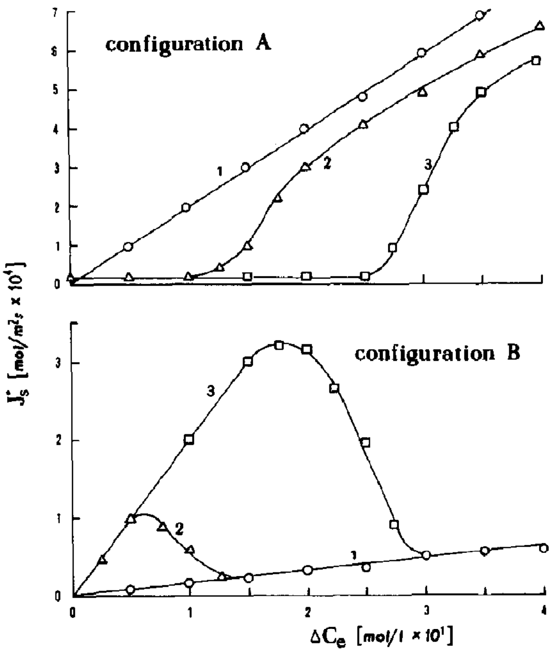

Fig. 7. Experimental and calculated ethanol flux across a cell membrane as a function of the ethanol concentration difference. Experiments were performed analogously to those for J_v^* (see fig. 5). Solid lines illustrate the solute flux calculated on the basis of eq. 28 after taking into consideration $\Omega_{22}(\Delta C_e)$.

two gravitational configurations of a single-membrane system. Let us consider the results shown in figs. 4–7. From these data we see that all dependences $J_v^* = f(\Delta C)$ and $J_s^* = f(\Delta C)$ for ternary solutions display non-linear behaviour. In order to apply eqs. 24–26 as well as eqs. 22 and 23 to a description of transmembrane transport in ternary solutions, the assumption of the Ω coefficients being dependent on the concentration and configuration is required. The pertinence of the above assumption is confirmed by the data on Ω_{11} and Ω_{22} in ternary solutions, shown in figs. 8 and 9.

In fig. 8, curves 1 and 2 represent the glucose concentration dependence of the coefficients Ω_{11} and Ω_{22} (at constant [ethanol]) for configuration A. In configuration B the patterns of glucose concentration dependence of Ω_{11} and Ω_{22} are inverted, as illustrated by curves 1 and 2. Both Ω_{11} and Ω_{22} depend on ethanol concentration (see curves 1 and 2, and 1* and 2* in fig. 9). Taking into consideration the concentration dependence of the coefficients Ω_{11} and Ω_{22}, demonstrated in figs. 8 and 9, and the values for the membrane parameters listed in table 2, the values of J_v^* and J_s^* as functions of the concentration differences, ΔC_g or ΔC_e, were calculated on the basis of eqs. 23–25. The solid lines in figs. 4–7 present the results calculated for J_v^* and J_s^*. One observes good agreement between the experimental data and the results from calculation. Therefore, eqs. 28–30, after taking into consideration the concentration dependence of $\Omega(C)$, yield satisfactory curve fitting to the experimental results.

If we assume that J_v^* and J_s^* are the generalized fluxes and ΔC a generalized thermodynamic force, the regions where $(\mathrm{d}J_v/\mathrm{d}C)$ or $(\mathrm{d}J_s/\mathrm{d}C)$ are decreased (see figs. 4–7) can be classified as the negative differential conductance regions. The phenomenon of negative conductance

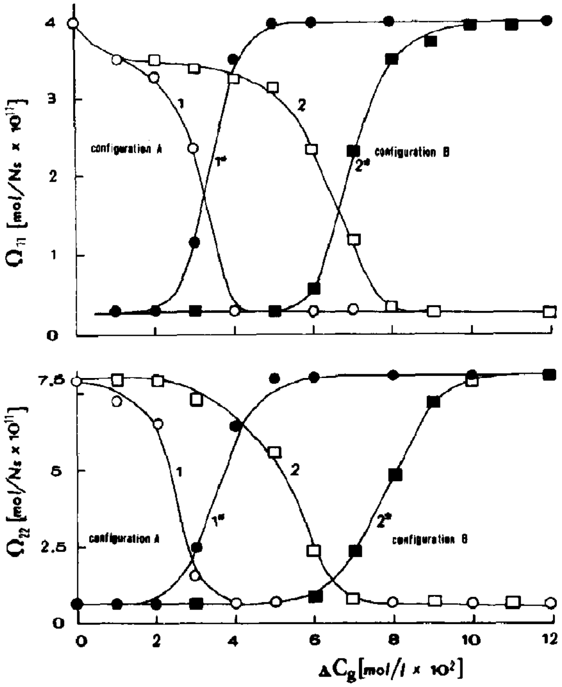

Fig. 8. Glucose concentration dependences of Ω_{11} (upper) in 0.2 M (curves 1 and 1*) and 0.4 M aqueous ethanol solution (curves 2 and 2*). Curves 1 and 2 correspond to configuration A; 1* and 2* to configuration B. (Lower panel) As above, but for Ω_{22}.

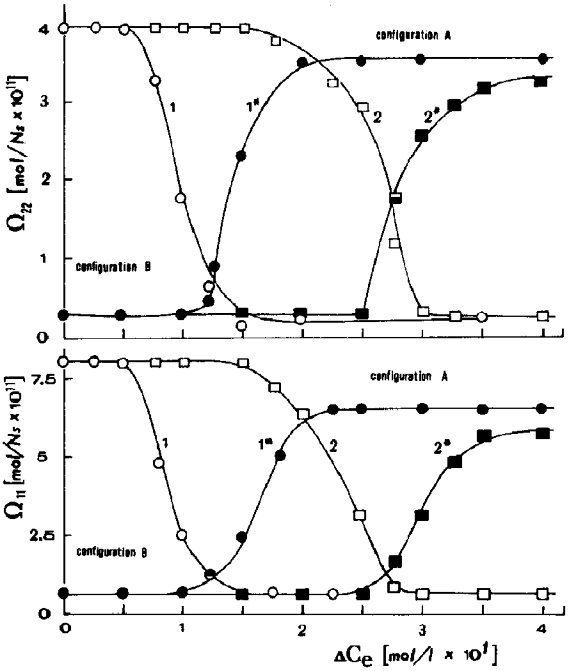

Fig. 9. Ethanol concentration dependence of Ω_{22} (upper) in 0.02 M (curves 1 and 1*) and 0.04 M aqueous glucose solution (curves 2 and 2*). Curves 1 and 2 refer to configuration A; 1* and 2* to configuration B. (Lower panel) Same as above, but for Ω_{11}.

appears in nature [46–48] and constitutes a very important factor in the physics of semiconductors [46], membranology [47] and in biophysics [48].

6. Gravitational effects of transport in a single-membrane system

Among the group of gravitational effects of transmembrane transport in membrane system examined in this paper, the following properties can be included: asymmetry and amplification of osmotic and diffusive transport. The problem of asymmetry of transport has been discussed in a previous paper [41]. The present article deals with the question as to the amplification of transmembrane transport (see below).

6.1. Amplification effect of osmotic transport

In order to discuss this effect we take into consideration curve 1, and curves 2, 3 illustrating the dependence $J_v^* = f(\Delta C_g)$ for binary and ternary solutions, respectively, presented in fig. 3. From analysis of the course of these variations in configuration B, it was determined that changes in J_v^* for binary solutions result from alterations in the glucose concentration $\Delta(\Delta C_g) = 0.01$ M and are identical throughout the entire range of glucose concentrations: $\Delta J_{v1} = 0.4 \times 10^{-8}$ m/s. In the case of ternary solutions, the variations in ΔJ_{v2} due to identical changes in concentration are different for various concentration ranges. The largest change in volume flux is $\Delta J_{v2}^{max} = 2.5 \times 10^{-8}$ m/s, 6-fold greater than the value of ΔJ_{v1}. In configuration A an identical change in glucose concentration in a binary solution was the result of changes of $\Delta J_{v2} = 0.5 \times 10^{-9}$ m/s and the maximal change in J_v^* in ternary solutions was $\Delta J_{v2}^{max} = -2.1 \times 10^{-8}$ m/s, being 42-fold greater than the value ΔJ_{v1}. The above means that the membrane system in both configurations is able to amplify the flux, and the formula

$$a_v = \frac{\Delta J_{v2}^{max}}{\Delta J_{v1}} \tag{31}$$

expresses the amplification coefficient of osmotic transport. From the values quoted for ΔJ_{v2}^{max} and ΔJ_{v1}, it can be determined that the single-membrane system in configuration B is characterized by a positive amplification coefficient, and in configuration A by a negative value.

6.2. Amplification effect of diffusive transport

In order to demonstrate this effect, let us now turn to a consideration of the dependence $J_s^* = f(\Delta C_g)$ for binary (curve 1) and ternary solutions (curves 2 and 3) depicted in fig. 6. Precisely as in the case of J_v^* in configuration B, changes in glucose flux for binary solutions are the consequence of variation in the glucose concentration $\Delta(\Delta C_g) = 0.01$ M and are identical over the whole range of glucose concentrations: $\Delta J_{s1} = 0.5 \times 10^{-5}$ mol/m^2 per s. In the case of ternary solutions,

Table 3

Values of the amplification coefficients of osmotic transport (a_v) and of diffusive transport (a_s)

Substance	Configuration	Amplification coefficient	
		a_v	a_s
Glucose	A	−42 ±3.0	−20 ±1.5
	B	5.0±0.3	3.1±0.2
Ethanol	A	4.5±0.3	3.1±0.8
	B	−42 ±3.0	−22 ±1.5

changes in ΔJ_{s2} due to identical variations in glucose concentrations vary according to the concentration range. The maximal change in glucose flux amounts to $\Delta J_{s2} = 1.53 \times 10^{-5}$ mol/m^2 per s, being 3-times larger than the value ΔJ_{s1} for binary solutions. In configuration A an analogous alteration in $\Delta(\Delta C_g)$ for binary solutions gives rise to an identical change in ΔJ_{s1} over the entire range of glucose concentrations. In this case, ΔJ_{s1} is equal to 0.1×10^{-5} mol/m^2 per s. The maximal change in J_s in ternary solutions is now $\Delta J_{s2}^{\max} = -2.0 \times 10^{-5}$ mol/m^2 per s, which is 10-fold greater than the value of ΔJ_{s1} for binary solutions. From the above, it is concluded that a single-membrane system in both gravitational configurations (A and B) possesses the property of amplification of diffusive flux. In turn, the following equation:

$$a_s = \frac{\Delta J_{s2}^{\max}}{\Delta J_{s1}} \tag{32}$$

defines the coefficient of amplification of diffusive transport. Using appropriate values for $\Delta J_{s2}^{\max}$ and ΔJ_{s1}, it can be shown that the single-membrane system is characterized by a positive amplification coefficient in configuration B, whereas it is negative for configuration A. The values of the osmotic and diffusive amplification coefficients are listed in table 3.

7. Conclusions

In this paper, it has been shown that the modified KKZ model may be applied to the interpretation of experimental results on transmembrane transport in multicomponent solutions. Nevertheless, application of this model is possible only when the concentration dependence of Ω_{ik} coefficients is known. The values of these coefficients depend on the hydrodynamic state of the boundary layer/membrane/boundary layer complex. A recent study [49] has shown that the expression describing coefficient Ω_{ik} should contain the Rayleigh number, the density and kinematic viscosity of the solutions, the acceleration due to gravity and the density gradient.

The effects of amplification described here and asymmetry of transmembrane transport reported previously [41] are indications of natural convection appearing or disappearing in the membrane system. These may be subdivided into a group of regulatory effects, including phenomena such as rectification, amplification and oscillation of transmembrane fluxes [50].

References

1 A. Fick, Pogg. Ann. 94 (1855) 59.

2 N. Laksminarayanaiah, Transport phenomena in membranes (Academic Press, New York, 1969).

3 J. Crank and G.S. Park, Diffusion in polymers (Academic Press, New York, 1968).

4 L.F. Del Castillo and E.A. Mason, Biophys. Chem. 12 (1980) 223.

5 E.A. Mason and L.A. Viehland, J. Chem. Phys. 68 (1978) 3562.

6 M.H. Friedman and R.A. Meyer, Biophys. J. 34 (1981) 535.

7 V.S. Vaidhyanathan and W.H. Perkins, J. Theor. Biol. 7 (1964) 329.

8 V.S. Vaidhyanathan, J. Theor. Biol. 7 (1964) 334.

9 K.S. Spiegler, Trans. Faraday Soc. 54 (1958) 1408.

10 O. Kedem and A. Katchalsky, J. Gen. Physiol. 45 (1961) 143.

11 L. Onsager, Phys. Rev. 37 (1931) 405.

12 O. Kedem and A. Katchalsky, Biochim. Biophys. Acta 27 (1958) 229.

13 A. Katchalsky and P.F. Curran, Nonequilibrium thermodynamics in biophysics (Harvard University Press, Cambridge, 1965).

14 O. Kedem and A. Katchalsky, Trans. Faraday Soc. 59 (1963) 1918.

15 O. Kedem and A. Katchalsky, Trans. Faraday Soc. 59 (1963) 1931.

16 O. Kedem and A. Katchalsky, Trans. Faraday Soc. 59 (1963) 1941.

17 C.R. House, Water transport in cells and tissues (Edward Arnold, London, 1974).

18 A.J. Staverman, Trans. Faraday Soc. 48 (1952) 176.
19 A. Zelman, Biophys. J. 12 (1972) 414.
20 I.W. Richardson, E.A.D. Foster and S. Miękisz, Bull. Math. Biol. 44 (1982) 761.
21 L.F. Del Castillo and E.A. Mason, J. Membrane Sci. 28 (1986) 229.
22 P.H. Barry and J.M. Diamond, Physiol. Rev. 64 (1984) 763.
23 J.M. Diamond and W.H. Bossert, J. Gen. Physiol. 50 (1967) 2061.
24 C.T. Everitt and D.A. Haydon, J. Theor. Biol. 22 (1969) 9.
25 K. Inenaga and H. Yoshida, J. Membrane Sci. 6 (1980) 271.
26 A. Rejou-Michel, M. Villardi and M. Delmotte, Bioelectrochem. Bioenerg. 104 (1979) 289.
27 A. Ślęzak, K. Dworecki and J.E. Anderson, J. Membrane Sci. 23 (1985) 71.
28 A. Ślęzak, J. Membrane Sci. 26 (1986) 115.
29 A. Ślęzak and B. Turczyński, Biophys. Chem. 24 (1986) 173.
30 A. Ślęzak and K. Dworecki, Stud. Biophys. 100 (1984) 41.
31 S. Przestalski and M. Kargol, Stud. Biophys. 34 (1972) 7.
32 M. Kargol, K. Dworecki and S. Przestalski, Stud. Biophys. 76 (1979) 137.
33 M. Kargol, Stud. Biophys. 80 (1980) 111.
34 A Ślęzak, Stud. Biophys. 88 (1982) 179.
35 M. Kargol, K. Dworecki and S. Przestalski, Stud. Biophys. 113 (1986) 31.
36 M. Kargol, Dyss. Hab. Pedagogical University of Kielce Press, Kielce (1978) (in Polish).
37 L. Brauner, Kolloidchem. Beih. 23 (1926) 143.
38 H.C. Custard and S.R. Faris, Planta 65 (1965) 183.
39 A. Ślęzak and B. Turczyński, Postępy Fiz. Med. 20 (1985) 253.
40 A. Ślęzak, Biophys. Chem. (1989) in the press.
41 A. Ślęzak and B. Turczyński, Stud. Biophys. 113 (1986) 37.
42 A. Ślęzak, B. Turczyński and Z. Nawrat, J. Non-Equilib. Thermodyn. 14 (1989) in the press.
43 A. Ślęzak, B. Turczyński and Z. Nawrat, in: Synthetic polymeric membranes, eds. B. Sedlacek and J. Kahovec (De Gruyter, Berlin, 1987) p. 445.
44 R.A. Meyer and M.H. Friedman, Rev. Sci. Instrum. 48 (1977) 1317.
45 A. Ślęzak and K. Dworecki, Postępy Fiz. Med. 19 (1984) 219.
46 W.H. Weber and G.W. Ford, Solid-State Electron. 13 (1970) 1333.
47 J.E. Anderson, J. Membrane Sci. 4 (1978) 35.
48 K.S. Cole, Membranes, ions and impulses (University of California Press, Berkeley, 1968).
49 A. Ślęzak, Biophys. Chem. (1989) submitted.
50 M. Kargol, A. Ślęzak and G. Suchanek, Postępy Fiz. Med. 16 (1981) 127.